Electronic Supplementary Material (ESI) for RSC Advances.
This journal is © The Royal Society of Chemistry 2022

Supporting Information:

Electrochemical performance of $CoSe_2$ with mixed phases decorated with N-doped rGO in Potassium-ion batteries

Hui Zheng[b,#], Han-Shu Xu[a,b,#,*], Jiaping Hu[b], Huimin Liu[b], Lianwei Wei[b], Shusheng Wu[b], Jin Li[b], Yuhu Huang[b] and Kaibin Tang[a,b,*]

[a] Hefei National Research Center for Physical Sciences at the Microscale, University of Science and Technology of China, Hefei, 230026, People's Republic of China

[b] Department of Chemistry, University of Science and Technology of China, Hefei, 230026, People's Republic of China

Corresponding authors

xhs@ustc.edu.cn

kbtang@ustc.edu.cn

Experimental section

1. Material synthesis

In a usual procedure, $Co(NO_3)_2 \cdot 6H_2O$ (55 mg) and PVP K-30 (350 mg) were added into deionized water (5 mL) and $CH_2(OH)_2$ (10 mL) with GO solution (2.93 mg/mL, 3.5mL) to form a uniform suspension. Meanwhile, selenium power (40 mg) was added into $C_2H_4(NH_2)_2$ (10 mL) to obtain a black solution. Then, these mixtures were mixed for 4 h under magnetically stirring. Afterward, the melange was placed into a 50 mL autoclave for reacting at 200 °C in 24 h. After centrifuging and washing with ethanol and deionized water, the $CoSe_2$@N-rGO nanoparticles were collected by freeze-dried. The $CoSe_2$ was prepared *via* a similar method with the synthesis of the $CoSe_2$@N-rGO product except adding GO solution.

2. Structural and morphological characterization

The powder X-ray diffraction (XRD) patterns were measured by using a SmartLab X-ray diffractometer (Cu-Kα1, λ = 1.5418Å). The scanning electron microscope (SEM) morphology were carried out by a field-emitting (FE) SEM (JEOL-JSM-6700F). Thermogravimetric analysis (TGA) was performed on a thermogravimetric analyser (GA Q5000IR) from 30 °C to 700 °C in air flow (50 mL/min) with a heating rate of 10 °C/min. The surface chemical state was determined by X-ray photoelectron spectroscopy (XPS, Thermo ESCALAB 250Xi), using Al Kα radiation. The Raman spectra were obtained using a Raman spectrophotometer (Horiba Jobin Yvon, HR800, France) in the range of 200-1800 cm^{-1} with 532 nm laser radiation. Brunauer−Emmett−Teller (BET) measurement was conducted in Quantachrome system with N_2 adsorption and desorption. High-resolution TEM (HRTEM) and energy-dispersive X-ray spectroscopy (EDX) mapping analyses were executed on a Talos F200X HRTEM supplied with a spherical aberration corrector.

3. Electrochemical tests

$CoSe_2$@N-rGO as an anode material for PIBs were assembled into CR 2032 coin-type half cells to investigate the electrochemical behavior. The working electrode was prepared by mixing 80 wt % active material with 10 wt % Super-p and 10 wt % CMC in water. The mixed slurry was coated on the copper foil and dried at 80 °C for 10 h in a vacuum oven. The mass loading of active materials was 0.96-1.17 mg cm^{-2}. The thin K metal sheet was used as the counter electrode and a GF/D glass microfiber was served as the separator. Moreover, a 1.0 M potassium bis(fluorosulfonyl)imide (KFSI) solution of dimethyl ether (DME) was applied as the electrolyte. The whole processes of battery making were carried out in a glove box filled with Ar gas ($O_2 \leq 0.01$ ppm; $H_2O \leq 0.01$ ppm). The electrochemical properties of electrodes were tested based on a multichannel battery testing system (Neware-BTS-TC53). The cyclic voltammograms (CV) at various scan rates and electrochemical impedance spectroscopy (EIS) in the frequency range of 0.01-100000 Hz were examined on an electrochemical workstation (CHI660E).

4. DFT Calculations

DFT calculations were performed using the CASTEP code of Materials Studio package of AccelrysInc[1]. Generalized gradient approximation (GGA) method and Perdew-Burke-Ernzerhof (PBE) functional were used to calculate the DFT exchange correlation energy. The core electrons were treated by ultra-soft pseudopotential (USP). The kinetic energy cutoff was set to 400 eV for

the plane-wave basis set and the self-consistent field (SCF) tolerance was 1×10^{-6} eV. 5×3×1 $CoSe_2$ surface built with a 20 Å vacuum region. The Brillouin zone was sampled by 4×4×1 Monkhorst-Pack mesh *k*-point for surface calculation and the DOS calculation.

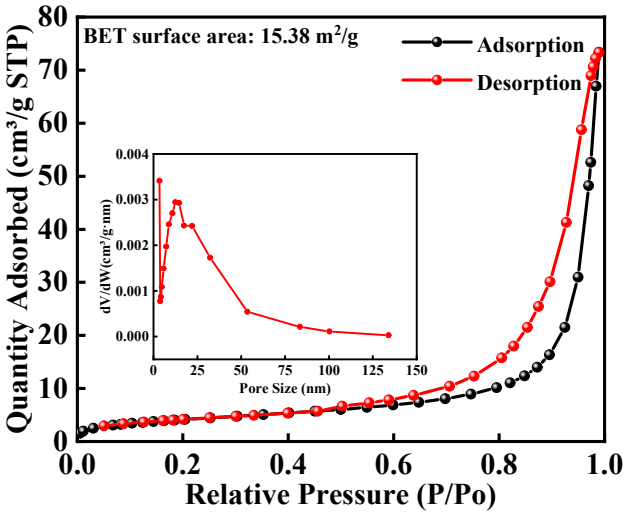

Fig. S1 Nitrogen adsorption/desorption profile and corresponding pore size distribution (inset map) of $CoSe_2$.

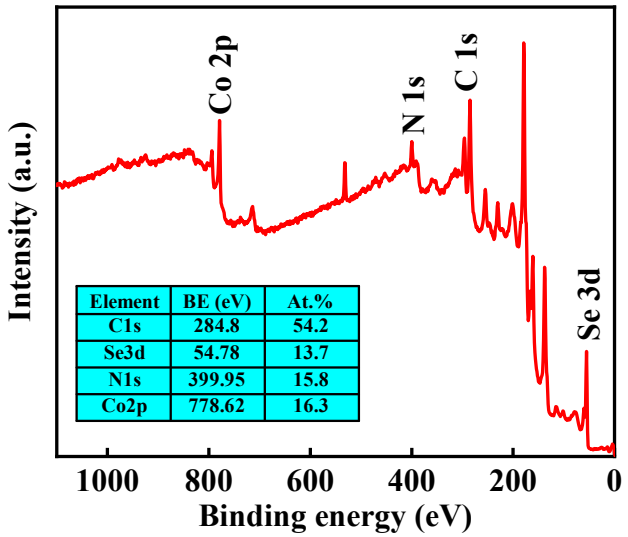

Element	BE (eV)	At.%
C1s	284.8	54.2
Se3d	54.78	13.7
N1s	399.95	15.8
Co2p	778.62	16.3

Fig. S2 XPS survey spectra of $CoSe_2$@N-rGO.

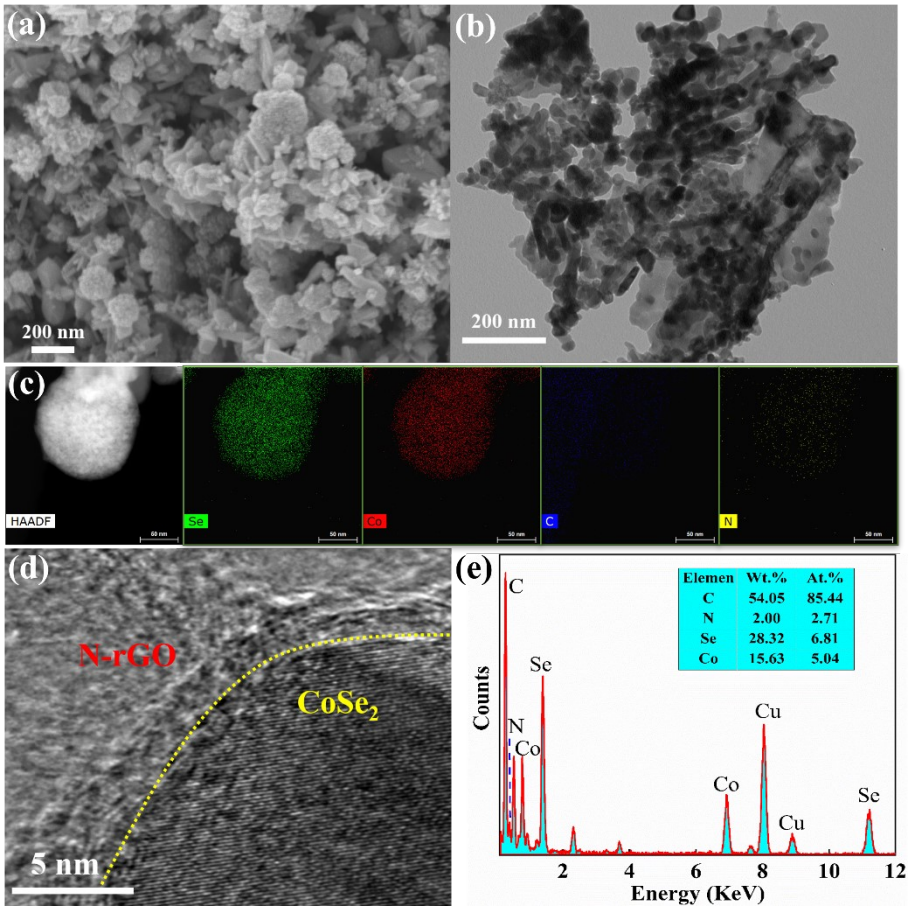

Fig. S3 (a-d) SEM, TEM, and EDS mapping of as-synthesized $CoSe_2$, (d) and (e) high-resolution TEM images and EDX spectra of as-synthesized $CoSe_2$@N-rGO. The signals of Cu in the spectrum comes from the copper grid.

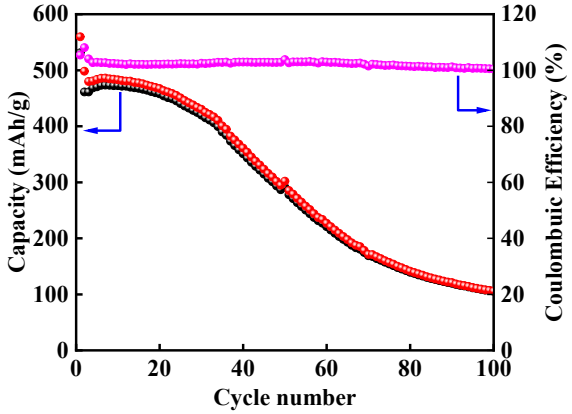

Fig. S4 Galvanostatic charge/discharge Capacity and Coulombic efficiency at a current density of 0.2 $A \cdot g^{-1}$ except for the initial cycle at 0.05 $A \cdot g^{-1}$ of $CoSe_2$.

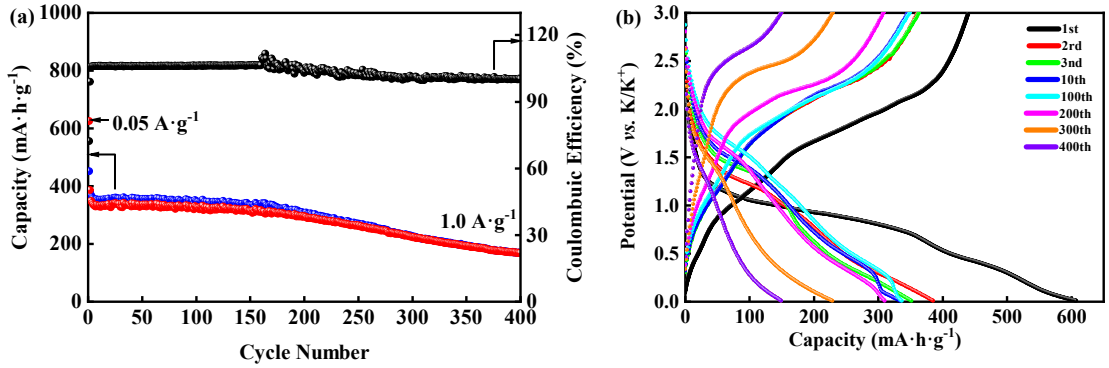

Fig. S5 (a) Long-term cycling stability and Coulombic efficiency of $CoSe_2$@N-rGO composites at a high current density of 1 $A \cdot g^{-1}$ except for the initial cycle at 0.05 $A \cdot g^{-1}$, (b) Charge/Discharge curves at 0.05 $A \cdot g^{-1}$ for initial cycle and 2rd, 3nd, 10th, 100th, 200th, 300th and 400th at 1 $A \cdot g^{-1}$.

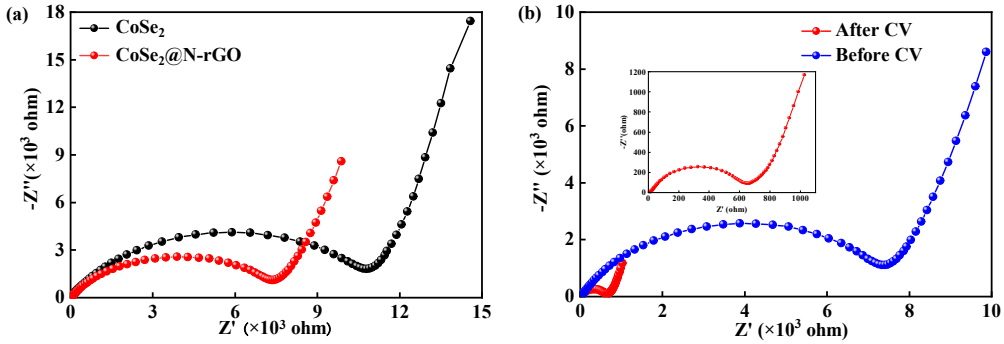

Fig. S6 (a) Comparison of electrochemical impedance spectroscopy (EIS) analysis of PIBs of both $CoSe_2$ electrode and $CoSe_2$@N-rGO electrodes; (b) Comparison of electrochemical impedance spectroscopy (EIS) analysis of fresh $CoSe_2$@N-rGO electrodes and cycled after CV.

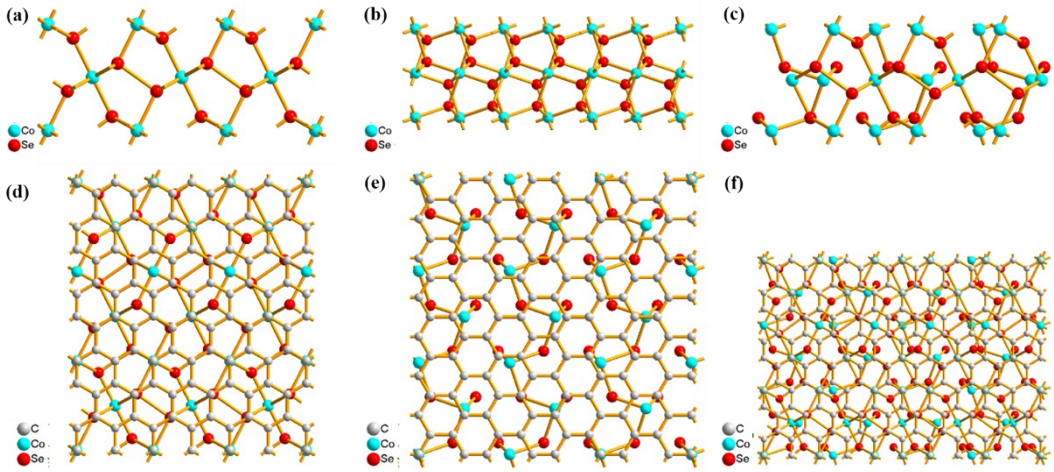

Fig.S7 The (001) surface image of (a) o-$CoSe_2$, (b) c-$CoSe_2$ and (c) o-$CoSe_2$/ c-$CoSe_2$, (d) o-$CoSe_2$@N-rGO, (e) c-$CoSe_2$@N-rGO and (f) o-$CoSe_2$/ c-$CoSe_2$@N-rGO. Here, o-$CoSe_2$ represent orthorhombic $CoSe_2$ and c-$CoSe_2$ represent cubic $CoSe_2$

Table S1. The electrochemical performance of $CoSe_2$@N-rGO and other anode materials for potassium-ion storage.

Materials	Cs (mA h/g)	Current density (A g^{-1})	Cycles (times)	Voltage Range (V *vs.* K^+ /K)	Crystal system	Ref.
$CoSe_2$–$MoSe_2$/rGO	498	0.1	60	0.01-3	Orthorhombic	2
$CoSe_2$⊂SPNC⊂rGO	208.8	0.5	500	0.01-3	Orthorhombic	3
$CoSe_2$@NC/MX	358	0.5	100	0.01-3	Cubic	4
	276	2.0				
Ni_3Se_4/$CoSe_2$@C	330.1	0.1	200	0.01-3	Cubic	5
$CoSe_2$@NC	311.3	0.05	1000	0.01-2.5	Cubic	6
	184.5	0.5				
$CoSe_2$@NC/rGO	226	0.5	400	0.01-2.5	Cubic & Orthorhombic	7
$CoSe_2$@NC/HMCS	442	0.1	120	0.01-3	Cubic & Orthorhombic	8
$CoSe_2$ threaded by N-doped carbon nanotubes	253	0.2	100	0.01-3	/	9
	173	2.0	600	0.01-3		
CoSe@NCNTs	282	0.2	500	0.01-3	/	10
CoSe@NrGo	143	0.2	100	0.01-3	/	11
CoSe@NC	309.6	0.2	500	0.01-3	/	12
CoSe@C/HCPs	182	0.3	300	0.01-3	/	13
$Co_{0.85}$Se-QDs/C	402	0.05	50	0.01-2.5	/	14
$Co_{0.85}$Se@NC	114.7	2.0	250	0.01-3	/	15
$CoSe_2$@N-rGO	421	0.2	100	0.01-3	Orthorhombic & Cubic	Our work
	174.69	1.0	400			

Table S2. The electrochemical performance of $CoSe_2$-derived anode materials for sodium-ion storage with difference crystal system

Materials	Cs (mA h/g)	Current density (A g^{-1})	Cycles (times)	Voltage Range (V *vs.* K^+ /K)	Crystal system	Ref.
$CoSe_2$@ CNTs–MXene	400	2	200	0.1-3	Cubic	16
$CoSe_2$@NC	395	0.5	200	0.01-3	Cubic	17
	367	2				
$CoSe_2$ HBs/$Ti_3C_2T_x$	186	0.5	3000	0.01-3	Cubic	18
Cu-doped $CoSe_2$ microboxes	492	0.05	/	0.01-3	Cubic	19
undoped $CoSe_2$ microboxes	480	0.05	/			
TNC-$CoSe_2$ microcubes	511	0.2	200	0.01-3	Cubic	20
	456	6.4	6000			
N-$CoSe_2$ yss	431	0.05	/	0.01-3	Cubic	21
Submicron Cobblestone-Like	414.6	0.2	700	0.5-3	Cubic	22
Carbon-Free $CoSe_2$	416.5	2.0	1350			
$CoSe_2$/Mo_2C/C NFs	530.7	0.1	100	0.01-3	Cubic	23
$CoSe_2$/ZnSe@C nanospheres	395	0.1	/	0.5-3	Orthorhombic	24
N-CNT/rGO/$CoSe_2$ NF	448	1.0	300	0.01-3	Orthorhombic	25
V-shaped $CoSe_2$@GR	549.4	0.1	/	0.01-3	Orthorhombic	26
$CoSe_2$@C∩NC	324	0.1	200	0.5-3	Orthorhombic	27
	234	5.0	2000			
multilayered yolk-shell $CoSe_2$ nano-dodecahedrons	352.9	1.0	2000	0.01-3	Orthorhombic	28
P-$CoSe_2$	206.9	2.0	1000	0.01-3	Orthorhombic	29
CS@PCNFs	413.6	0.2	150	0.01-3	Orthorhombic	30
	401.5	2.0	/			
$CoSe_2$@N-CF/CNTs	428	1.0	500	0.01-3	Orthorhombic	31
CNT/$CoSe_2$@NC	404	0.2	120	0.01-3	Cubic & Orthorhombic	32
$CoSe_2$@NPGC/CNTs	424	0.2	100	0.01-3	Cubic & Orthorhombic	33
$CoSe_2$@AC	100	0.2				

References

(1) Clark, S. J.; Segall, M. D.; Pickard, C. J.; Hasnip, P. J.; Probert, M. I.; Refson, K.; Payne, M. C. First principles methods using CASTEP. *Zeitschrift für kristallographie-crystalline materials* **2005,** *220*, 567-570.

(2) Xu, Y.; Liu, X.; Su, H.; Jiang, S.; Zhang, J.; Li, D. Hierarchical Bimetallic Selenides $CoSe_2$-$MoSe_2$/rGO for Sodium/Potassium-Ion Batteries Anode: Insights into the Intercalation and Conversion Mechanism. *Energy & Environmental Materials* **2022**, *5*, 627-636.

(3) Zhao, Z.; Gao, C.; Fan, J.; Shi, P.; Xu, Q.; Min, Y. Dual Confinement of $CoSe_2$ Nanorods with Polyphosphazene-Derived Heteroatom-Doped Carbon and Reduced Graphene Oxide for Potassium-Ion Batteries. *ACS Omega* **2021**, 6, 17113-17125.

(4) Oh, H. G.; Yang, S. H.; Kang, Y. C.; Park, S. K. N-doped carbon-coated $CoSe_2$ nanocrystals anchored on two-dimensional MXene nanosheets for efficient electrochemical sodium-and potassium-ion storage. *International Journal of Energy Research* **2021**, 45, 17738-17748.

(5) Zhang, Y.; Wei, S.; Zhao, Z.; Pei, X.; Zhao, W.; Wang, J.; Du, X.; Li, D. Carbon-Encapsulated Ni_3Se_4/$CoSe_2$ Heterostructured Nanospheres: Sodium/Potassium-Ion Storage Anode with Prominent Electrochemical Properties. *Small* **2022**, e2107258.

(6) Hu, J.; Wang, B.; Yu, Q.; Zhang, D.; Zhang, Y.; Li, Y.; Wang, W. A. $CoSe_2$/N-doped carbon porous nanoframe as an anode material for potassium-ion storage. *Nanotechnology* **2020**, 31, 395403.

(7) Zhao, J.; Wu, H.; Li, L.; Lu, S.; Mao, H.; Ding, S. A $CoSe_2$-based 3D conductive network for high-performance potassium storage: enhancing charge transportation by encapsulation and restriction strategy. *Materials Chemistry Frontiers* **2021**, 5, 5351-5360.

(8) Yang, S. H.; Park, S. K.; Kang, Y. C. MOF-Derived $CoSe_2$@N-Doped Carbon Matrix Confined in Hollow Mesoporous Carbon Nanospheres as High-Performance Anodes for Potassium-Ion Batteries. *Nanomicro Lett* **2021**, 13, 1-15.

(9) Yu, Q.; Jiang, B.; Hu, J.; Lao, C. Y.; Gao, Y.; Li, P.; Liu, Z.; Suo, G.; He, D.; Wang, W. A.; Yin, G. Metallic Octahedral $CoSe_2$ Threaded by N-Doped Carbon Nanotubes: A Flexible Framework for High-Performance Potassium-Ion Batteries. *Adv Sci* **2018**, 5, 1800782.

(10) Liu, Y.; Deng, Q.; Li, Y.; Li, Y.; Zhong, W.; Hu, J.; Ji, X.; Yang, C.; Lin, Z.; Huang, K. CoSe@N-Doped Carbon Nanotubes as a Potassium-Ion Battery Anode with High Initial Coulombic Efficiency and Superior Capacity Retention. *ACS Nano* **2021**, 15, 1121-1132.

(11) Liu, Y.; Cui, K.; Ma, Z.; Wang, X. Pseudocapacitance-Induced High-Rate Potassium Storage in CoSe@NrGo Hybrid Nanosheets for Potassium-Ion Batteries. *Energy & Fuels* **2020**, 34, 10196-10202.

(12) Huang, Q.; Fan, X.; Ou, X.; Wang, H.; Wu, L.; Yang, C. Fabrication of CoSe@NC nanocubes for high performance potassium ion batteries. *J Colloid Interface Sci* **2021**, 604, 157-167.

(13) Zhang, Z.; Zhang, B.; Xu, J.; Zhang, M.; Duan, L.; Shen, J.; Zhou, X. Anchoring Carbon-Coated CoSe Nanoparticles on Hollow Carbon Nanocapsules for Efficient Potassium Storage. *ACS Applied Energy Materials* **2021**, 4, 6356-6363.

(14) Liu, Z.; Han, K.; Li, P.; Wang, W.; He, D.; Tan, Q.; Wang, L.; Li, Y.; Qin, M.; Qu, X. Tuning Metallic $Co_{0.85}Se$ Quantum Dots/Carbon Hollow Polyhedrons with Tertiary Hierarchical Structure for High-Performance Potassium Ion Batteries. *Nanomicro Lett* **2019**, 11, 1-14.

(15) Ma, G.; Li, C.; Liu, F.; Majeed, M. K.; Feng, Z.; Cui, Y.; Yang, J.; Qian, Y. Metal-organic framework-derived $Co_{0.85}Se$ nanoparticles in N-doped carbon as a high-rate and long-lifespan anode material for potassium ion batteries. *Materials Today Energy* **2018**, 10, 241-248.

(16) Xu, E.; Li, P.; Quan, J.; Zhu, H.; Wang, L.; Chang, Y.; Sun, Z.; Chen, L.; Yu, D.; Jiang, Y.

Dimensional Gradient Structure of $CoSe_2$@CNTs-MXene Anode Assisted by Ether for High-Capacity, Stable Sodium Storage. *Nanomicro Lett* **2021**, 13, 1-14.
(17) Liu, T.; Li, Y.; Hou, S.; Yang, C.; Guo, Y.; Tian, S.; Zhao, L. Building Hierarchical Microcubes Composed of One−Dimensional $CoSe_2$@ Nitrogen−Doped Carbon for Superior Sodium Ion Batteries. *Chemistry-A European Journal* **2020**, 26, 13716-13724.
(18) Zhang, L.; Liu, W.; Ma, Q.; Xu, Y.; Liu, Z.; Wang, G. Electrostatic self-assembly synthesis of $CoSe_2$ HBs/ $Ti_3C_2T_x$ composites for long-cycle-life sodium ion batteries. *ChemElectroChem* **2021**, 8, 4047-4053.
(19) Fang, Y.; Yu, X. Y.; Lou, X. W. D. Formation of Hierarchical Cu-Doped $CoSe_2$ Microboxes via Sequential Ion Exchange for High-Performance Sodium-Ion Batteries. *Adv Mater* **2018**, 30, e1706668.
(20) Zhao, H.; Qi, Y.; Liang, K.; Li, J.; Zhou, L.; Chen, J.; Huang, X.; Ren, Y. Interface-Driven Pseudocapacitance Endowing Sandwiched $CoSe_2$/N-Doped Carbon/TiO_2 Microcubes with Ultra-Stable Sodium Storage and Long-Term Cycling Stability. *ACS Appl Mater Interfaces* **2021**, 13, 61555-61564.
(21) Geng, J.; Zhang, S.; Ang, E. H.; Guo, J.; Jin, Z.; Li, X.; Cheng, Y.; Dong, H.; Geng, H. Modulating the kinetics of $CoSe_2$ yolk–shell spheres via nitrogen doping with high pseudocapacitance toward ultra-high-rate capability and high-energy density sodium-ion half/full batteries. *Materials Chemistry Frontiers* **2021**, 5, 6873-6882.
(22) Liu, T.; Hou, S.; Li, Y.; Guo, Y.; Yang, C.; Zhao, L. Tailoring Submicron Cobblestone-Like Carbon-Free $CoSe_2$ with High Energy Density for Sodium-Ion Batteries. *ACS Applied Energy Materials* **2020**, 3, 9558-9567.
(23) Yang, J.; Yuan, W.; Zhou, X.; Zhang, Y.; Zheng, Y.; Yan, Q.; Liu, Y.; Dong, X. Nano-confined $CoSe_2$/Mo_2C nanoparticles encapsulated into porous carbon nanofibers for superior lithium and sodium storage. *Materials Today Energy* **2018**, 10, 317-324.
(24) Xiao, D.; Liu, S.; Zhao, K.; Ye, G.; Su, Y.; Zhu, W.; He, Z. Metal-organic framework-derived ultrasmall nitrogen-doped carbon-coated $CoSe_2$/ZnSe nanospheres as enhanced anode materials for sodium-ion batteries. *Ionics* **2021**, 27, 3327-3337.
(25) Jo, M. S.; Lee, J. S.; Jeong, S. Y.; Kim, J. K.; Kang, Y. C.; Kang, D. W.; Jeong, S. M.; Cho, J. S. Golden Bristlegrass-Like Hierarchical Graphene Nanofibers Entangled with N-Doped CNTs Containing $CoSe_2$ Nanocrystals at Each Node as Anodes for High-Rate Sodium-Ion Batteries. *Small* **2020**, 16, e2003391.
(26) Xiao, Y.; Zhang, J.; Su, D.; Zhang, A.; Jin, Q.; Zhou, L.; Wu, S.; Wang, X.; Chen, W.; Fang, S. *In-situ* growth of V-shaped $CoSe_2$ nanorods on graphene with C-Co bonding for high-rate and long-life sodium-ion batteries. *Journal of Alloys and Compounds* **2020**, 819, 153359.
(27) Li, B.; Liu, Y.; Jin, X.; Jiao, S.; Wang, G.; Peng, B.; Zeng, S.; Shi, L.; Li, J.; Zhang, G. Designed Formation of Hybrid Nanobox Composed of Carbon Sheathed $CoSe_2$ Anchored on Nitrogen-Doped Carbon Skeleton as Ultrastable Anode for Sodium-Ion Batteries. *Small* **2019**, 15, e1902881.
(28) Liang, H.; Li, X.; Liu, X.; Sun, R.; Qin, Z.; Zhang, Y.; Fan, H. Epitaxial growth induced multilayer yolk-shell structured $CoSe_2$ with promoting transport kinetics of sodium ion half/full batteries. *Journal of Power Sources* **2022**, 517, 230729.
(29) Ye, J.; Li, X.; Xia, G.; Gong, G.; Zheng, Z.; Chen, C.; Hu, C. P-doped $CoSe_2$ nanoparticles embedded in 3D honeycomb-like carbon network for long cycle-life Na-ion batteries. *Journal of Materials Science & Technology* **2021**, 77, 100-107.
(30) Li, F.; Li, L.; Yao, T.; Liu, T.; Zhu, L.; Li, Y.; Lu, H.; Qian, R.; Liu, Y.; Wang, H. Electrospinning synthesis of porous carbon nanofiber supported $CoSe_2$ nanoparticles towards enhanced sodium ion

storage. *Materials Chemistry and Physics* **2021**, 262, 124314.
(31) Yang, J.; Gao, H.; Men, S.; Shi, Z.; Lin, Z.; Kang, X.; Chen, S. $CoSe_2$ Nanoparticles Encapsulated by N-Doped Carbon Framework Intertwined with Carbon Nanotubes: High-Performance Dual-Role Anode Materials for Both Li- and Na-Ion Batteries. *Adv Sci* **2018**, 5, 1800763.
(32) Yousaf, M.; Chen, Y.; Tabassum, H.; Wang, Z.; Wang, Y.; Abid, A. Y.; Mahmood, A.; Mahmood, N.; Guo, S.; Han, R. P. S.; Gao, P. A Dual Protection System for Heterostructured 3D CNT/$CoSe_2$/C as High Areal Capacity Anode for Sodium Storage. *Adv Sci* **2020**, 7, 1902907.
(33) Park, S.-K.; Kim, J. K.; Kang, Y. C. Excellent sodium-ion storage performances of $CoSe_2$ nanoparticles embedded within N-doped porous graphitic carbon nanocube/carbon nanotube composite. *Chemical Engineering Journal* **2017**, 328, 546-555.
(34) Cui, C.; Wei, Z.; Zhou, G.; Wei, W.; Ma, J.; Chen, L.; Li, C. Quasi-reversible conversion reaction of $CoSe_2$/nitrogen-doped carbon nanofibers towards long-lifetime anode materials for sodium-ion batteries. *Journal of Materials Chemistry A* **2018**, 6, 7088-7098.